Design and Control of Wearable Ankle Robotic Device

Ali Zakaria Messaoui[1], Mohamed Amine Alouane[1], Mohamed Guiatni[1], Omar Mechali[2], Sbargoud Fazia[1], Zerdani Serine[1] and Belimene Cheikh Elmokhtar[1]
[1]*Complex Systems Control and Simulators Laboratory, Ecole Militaire Polytechnique, Bordj El Bahri, Algiers, Algeria*
[2]*Ecole Supérieur Ali Chabati, Reghaia, Algiers, Algeria*

Keywords: Exoskeleton Robot, Gait Assistance, Ankle Wearable Device Design, Finite-Time Stability, Homogeneous Sliding Mode Control.

Abstract: The primary objective of this paper is to develop an ankle wearable robotic device, which involves two primary tasks: design and control. The design task focused on creating a comfortable, lightweight, and secure ankle exoskeleton robot; this task was achieved using SOLIDWORKS and considering all essential factors. For the control aspect of the exoskeleton, an Improved Optimized Homogeneous Twisting Control (IOHTC) approach was proposed to design a robust angular position control system. To ensure the stability of the control system, a homogeneous-Lyapunov function was used. Simulation results based on real gait data demonstrated consistency with the theoretical foundation, and a comparative analysis based on various performance indices confirmed the effectiveness and superiority of the proposed control law. Finally, several simulations have been conducted on the designed model using simscape multibody link to validate it.

1 INTRODUCTION

Exoskeleton robots are mechanical devices that human operators wear to enhance their physical capabilities. These robots are commonly referred to as wearable robots or powered exoskeletons. They are categorized based on their applications, including medical and rehabilitation, industrial, military, and defence.

Medical and rehabilitation exoskeletons (Plaza, 2021) are designed to assist people with mobility impairments caused by neurological or muscular disorders, spinal cord injuries, or other conditions. These exoskeletons provide support for walking, standing, and other daily activities. On the other hand, industrial exoskeletons (De Looze, 2016) are designed to reduce the risk of injury and fatigue in workers who perform tasks such as heavy lifting and repetitive motions. Lastly, military and defence exoskeletons (Farris, 2023) improve soldiers' physical performance by providing increased strength, agility, and endurance.

The applications of exoskeleton robots are diverse and range from rehabilitation and physical therapy to injury prevention and augmented reality (Mubin, 2019). Exoskeletons are used to assist patients in regaining mobility and improving their physical capabilities. Industrial exoskeletons can reduce the risk of workplace injuries and assist workers when doing demanding tasks. Additionally, exoskeletons can be used for exploration and rescue operations, as well as for gaming and training purposes with augmented reality technology.

Ankle wearable robotic device is a valuable subclass of exoskeleton robots that provides support and assistance with ankle movements for various populations, including patients, athletes, and soldiers (Plaza, 2021). It is a frame that attaches to the lower leg and foot with a motorized joint that mimics the movement of the ankle. The device is programmable to assist with specific movements such as dorsiflexion and plantarflexion.

Ankle exoskeleton robots have a broad range of applications. It is primarily used in medical rehabilitation for patients with ankle injuries or neurological disorders such as cerebral palsy, multiple sclerosis, or stroke. Additionally, athletes can use it to enhance performance and prevent injuries during physical activities. Lastly, it has military and defence applications, where it can help soldiers enhance their endurance and walk and run faster during military operations.

The design of ankle exoskeleton robots must consider several factors, including comfort, safety, usability, and effectiveness (Lee, 2021). Some examples of existing ankle exoskeleton robots include:

Messaoui, A., Alouane, M., Guiatni, M., Mechali, O., Fazia, S., Serine, Z. and Elmokhtar, B.
Design and Control of Wearable Ankle Robotic Device.
DOI: 10.5220/0012157200003543
In *Proceedings of the 20th International Conference on Informatics in Control, Automation and Robotics (ICINCO 2023) - Volume 1*, pages 554-561
ISBN: 978-989-758-670-5; ISSN: 2184-2809

- H2 Ankle Exoskeleton is designed to assist with ankle movement and improve balance and stability for individuals with neurological or muscular disorders (Bortole, 2015). It is worn like a brace and provides adjustable levels of support for different activities.
- Ankle Assist Robot is developed to assist with ankle dorsiflexion and plantarflexion for individuals with limited ankle mobility. It is worn like a shoe and uses pneumatic actuators to assist with ankle movement (Alvarez-Perez, 2020).
- Ankle Rehabilitation Exoskeleton (ARES) is constructed to assist with ankle dorsiflexion and plantarflexion for individuals rehabilitating for ankle injuries or conditions. It is worn like a brace and provides adjustable levels of support for different stages of rehabilitation (Plaza, 2021).

In medical and rehabilitation applications, the control strategy is essential because the robot must adapt to each patient's needs. The control strategy must be capable of adjusting the level of assistance provided by the exoskeleton based on the patient's condition and progression. Additionally, the control strategy must ensure that the robot is not impeding the patient's natural movements and is not causing discomfort or pain. Sliding Mode Control (SMC) (Mechali, 2022) (Messaoui, 2023), among other robust control approaches, is an active topic in the exoskeleton robot's community nowadays for controlling ankle exoskeleton robot (Zhao, 2021). The simplicity of design and the fast response are among the benefits of such methods. In addition, it accurately compensates for matched disturbances. Several recent research works have focused on synthesizing and implementing robust SMC-based control laws for disturbance handling in wearable robotic devices (Pont-Esteban, 2022).

The main scientific contributions of the current research can be summed up as follows:

- The design of an ankle wearable robotic device for gait assistance applications;
- Inspired by the homogeneity theory, an IOHTC is proposed to deal with the fast dynamics' response of the joint angle position during gait. The proposed controller allows for mitigating the chattering of discontinuous SMC techniques;
- It is worth mentioning that the disturbance rejection does not require the design of an observer or an adaptation mechanism since the control law integrates a compensation term.
- In terms of validation, first, several simulations of the proposed control were conducted. The proposed controller was applied to the designed ankle exoskeleton using a simscape multibody link, and finally, the suggested IOHTC method and two other controllers are compared in this study.

The rest of this paper is organized as follows: the second section presents the design of the ankle exoskeleton robot; the third section introduces the proposed control technique and control law synthesis; the fourth section presents and discusses the different simulation results; and finally, section five concludes this paper and shows the future directions.

2 ANKLE EXOSKELETON PRESENTATION AND DESIGN

2.1 Ankle Exoskeleton Presentation

The proposed ankle exoskeleton robot is designed to assist the wearer during walking and daily life tasks, so this robot is intended for people who have a weakness of the lower limb muscles that can affect the movement of the ankle, which may cause abnormalities during gait, or for people who have an ankle dysfunction due to neurological or stroke disorders.

Therefore, the ankle exoskeleton robot should be as light as possible, compatible with the wearer's ankle and not interfere with the natural movement desired by the user. Inspired by the movement of the human ankle during walking, the design aims to propose a structure of an exoskeleton robot that is compatible with the natural movement of the human ankle in order to assist walking in patients who have muscle weakness in the lower limbs.

2.2 Ankle Exoskeleton Design

Generally, the human ankle has three degrees of rotational freedom (Fig.1). Primarily, the dorsiflexion/plantarflexion movement is the dominant movement during walking and even during most daily life tasks. Therefore, the proposed structure for designing the ankle exoskeleton robot has only one motorized joint to assist gait.

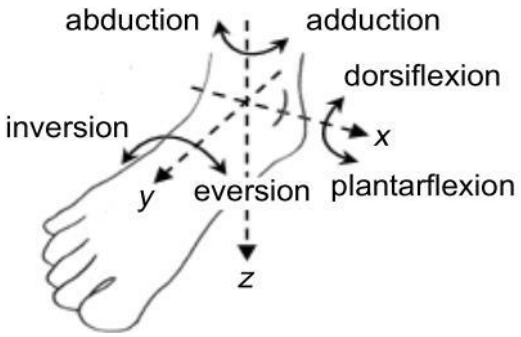

Figure 1: Human ankle morphological motion.

The dorsiflexion/plantarflexion movement of the exoskeleton robot is ensured by a MAXON DC motor equipped with a HEDL-5540-A12 encoder to close the control loop. In order to increase the torque generated by the motor, a reduction chain composed of several gears and a worm gear has been implemented (Fig.2). It is important to note that the foot support is equipped with force sensors (FSR) that serve to detect the different phases of walking; other force sensors will be placed between the foot of the wearer and the attaches that fix the foot with the foot support as a safety standard (a threshold of interaction force not to exceed).

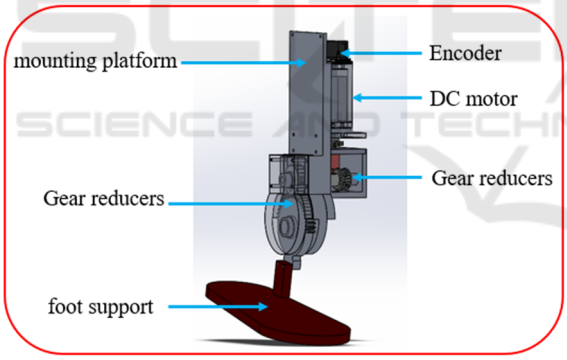

Figure 2: Designed ankle exoskeleton robot.

3 ANKLE EXOSKELETON ROBOT CONTROL

The specific type of control used for the ankle exoskeleton robot will depend on various factors, including the intended use of the exoskeleton, the target user population, and the device's technical specifications. Position control, velocity control, and torque control are three standard methods of controlling the movement of an ankle exoskeleton robot. Position control: In position control, the exoskeleton has to maintain a specific position or range of motion at the ankle joint; this kind of control is helpful for applications where precise movement is required, such as walking or standing. Velocity control: In velocity control, the exoskeleton is programmed to maintain a specific speed or rate of movement at the ankle joint. Velocity control is practical for applications requiring a specific speed or gait pattern, such as walking or running. Torque control: the exoskeleton must reach a specific torque or force output at the ankle joint. Torque control is advantageous for applications where the user needs assistance with tasks that require a certain level of force, such as lifting or carrying heavy objects.

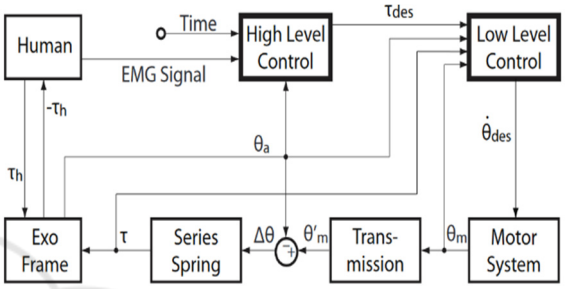

Figure 3: The exoskeleton robot control levels.

Generally, to ensure a good user experience and a safe human-robot interaction, three levels of ankle exoskeleton robot control work together (Fig.3), including:

1. Low-level control: This control involves the primary control of the exoskeleton's hardware components, such as the motor, sensors, and actuators. The low-level control typically includes tasks such as signal processing, filtering, and amplifying sensor signals, as well as motor control algorithms for controlling the exoskeleton's movement.
2. Mid-level control: This level of control involves coordinating the exoskeleton's movements with the user's movement. The mid-level control typically includes gait pattern recognition, motion planning, and trajectory generation. Mid-level control aims to ensure that the exoskeleton moves in a natural and
3. coordinated way with the user's own movements.
4. High-level control: This level of control involves overall system management and decision-making. The high-level control typically includes user intention recognition, task-level planning, and human-machine interface design. High-level control aims to ensure that the exoskeleton operates safely and

efficiently while providing the user with the intended level of assistance.

This work will focus on low-level position control of the proposed ankle exoskeleton robot. For this purpose, we propose using Improved Optimized Homogeneous Twisting Control (IOHTC) for ankle trajectory tracking during gait.

3.1 Preliminaries

Lemma 1. (Xu, 2017). Consider the following system

$$\dot{x} = f(x), \quad x(0) = x_0, x \in \mathbb{R}^n \tag{1}$$

If there exist C^1 Lyapunov function $V(x)\colon \mathrm{D} \to \mathbb{R}_+$ and some real constants $0 < c < \infty$ and $0 < \alpha < 1$, such that $\dot{V}(x) \le -cV(x)^\alpha$, then system (1) is finite-time stable for any given $x(t_0) \in \mathrm{D}_0 \subseteq \mathrm{D}$.

3.2 Control Problem Statement

The differential equations governing the actuator dynamics of the exoskeleton in the presence of external disturbances are given as:

$$\left\{\ddot{\theta} = \frac{k}{RJ}\left[u_\theta - \left(\frac{Rb}{k} + k\right)\dot{\theta} + d_\theta^{ext}\right]\right. \tag{2}$$

Where R, k, J, b are the actuator parameters, and θ presents the actuation angular position. In order to elaborate an adequate control model of the actuator, state-space representation can be used to reformulate the mathematical model as

$$\begin{cases}\dot{\mathrm{x}}_1 = \mathrm{x}_2, \\ \dot{\mathrm{x}}_2 = \dfrac{k}{RJ}\left(-\left(\dfrac{Rb}{k} + k\right)\dot{\theta} + u_\theta + d_\theta^{ext}\right),\end{cases} \tag{3}$$

where $\mathrm{x} \triangleq^{\text{def}} [\theta \quad \dot{\theta}] \in \mathbb{R}^2$ is the state vector. Consequently, the design of the control law follows from the perturbated second-order nonlinear system below:

where $X_\theta \triangleq^{\text{def}} [\chi_1 \quad \chi_2]^T \in \mathbb{R}^2$ is the vector of states, and $\chi_1 \triangleq^{\text{def}} \theta$, $\chi_2 \triangleq^{\text{def}} \dot{\theta}$, $u_\theta \triangleq^{\text{def}} V \in \mathbb{R}$ is the control input, $\mathcal{Y}_1 \triangleq^{\text{def}} \theta \in \mathbb{R}$ is the controlled output, and the uncertain function $d_\theta^{\mathrm{lum}} \in \mathbb{R}$ stands for the total lumped disturbances, i.e., unmodeled dynamics and external load perturbations. The functions $f_\theta(\chi_2, t), g_\theta$ are defined as:

$$\begin{cases}\dot{\chi}_1(t) = \chi_2(t), \\ \dot{\chi}_2(t) = f_\theta(\chi_2, t) + g_\theta u_\theta(t) \\ \quad + d_\theta^{lum}(d_\theta^{ext}, d_\theta^{unm}, t), \\ \mathcal{Y}_1(t) = \chi_1(t)\end{cases} \tag{4}$$

$$f_\theta(\chi_2, t) = -\frac{Rb + k^2}{RJ}\dot{\theta}(t).\, g_\theta \triangleq^{\text{def}} \frac{k}{RJ} \tag{5}$$

Definition 1. (Robust tracking control problem). The considered control problem of our study consists of designing robust finite-time SMC laws $\boldsymbol{u_\theta}$ for the position control affected by perturbations in (4), such that: ***(i)*** The position tracking error tend to the origin in finite-time, i.e., for $\forall \boldsymbol{e_1^\theta(t)} \triangleq^{\text{def}} \boldsymbol{\theta(t) - \theta_d(t)}$, there exist a constant $\boldsymbol{T_\theta}$, such that: $\lim_{t \to T_\theta} \boldsymbol{e_1^\theta(t) = 0}$, $\forall \boldsymbol{t > T_\theta}$, where $\boldsymbol{\theta_d}$ is the desired reference signal for the position system. ***(ii)*** The controller must ensure robustness against uncertainties and disturbances. ***(iii)*** The control signal is chattering-free.

3.3 Control Design and Stability Analysis

3.3.1 Control Design

Let the position tracking error and its dynamics be defined as

$$\begin{cases}e_1^\theta(t) \triangleq^{\text{def}} \theta(t) - \theta_d(t), \\ e_2^\theta(t) \triangleq^{\text{def}} \dot{\theta}(t) - \dot{\theta}_d(t).\end{cases} \tag{6}$$

The derivatives of the above expressions are given as

$$\begin{cases}\dot{e}_1^\theta = e_2^\theta, \\ \dot{e}_2^\theta = \ddot{\theta} - \ddot{\theta}_d.\end{cases} \tag{7}$$

The basic Twisting Control (TC) algorithm is given as

$$\begin{cases}\bar{u}_\theta = -k_{\theta_1}\left\lceil e_1^\theta \right\rfloor^{\frac{1}{3}} - k_{\theta_2}\left\lceil e_2^\theta \right\rfloor^{\frac{1}{2}} + \vartheta_\theta, \\ \dot{\vartheta}_\theta = -k_{\theta_3}\left\lceil e_1^\theta \right\rfloor^{0} - k_{\theta_4}\left\lceil e_2^\theta \right\rfloor^{0}.\end{cases} \tag{8}$$

Remark 1. It has been shown in work (Falcón R. R., 2019) that the TC controller generates a higher frequency, i.e., chattering, in its control signal, which limits its application in practice. Therefore, to improve its performance, we propose to: ***(i)*** Design a smooth hyperbolic function to mitigate the chattering effect as $\mathcal{H}(e_1^\theta) \triangleq^{\text{def}} (e_1^\theta)^{\varpi}[\tanh(e_1^\theta/v)]^{\varpi}$, and $\mathcal{H}(s_\theta) \triangleq^{\text{def}} (s_\theta)^{\varpi}[\tanh(s_\theta/v)]^{\varpi}$; ***(ii)*** Integrate the following sliding function s_θ in the basic TC's algorithm: $s_\theta = e_2^\theta + k_s e_1^\theta$ to enhance its robustness.

Therefore, by introducing the following control law for the actuator system

$$\begin{cases}\bar{u}_\theta \triangleq^{\text{def}} -k_{\theta_1}\left|e_1^\theta\right|^{\frac{1}{3}}\mathcal{H}(e_1^\theta) \\ \qquad -k_{\theta_2}|s_\theta|^{\frac{1}{2}}\mathcal{H}(s_\theta) + \vartheta_\theta, \\ \dot{\vartheta}_\theta \triangleq^{\text{def}} -k_{\theta_3}\left|e_1^\theta\right|^{0}\mathcal{H}(e_1^\theta) \\ \qquad -k_{\theta_4}|s_\theta|^{0}\mathcal{H}(s_\theta), \\ s_\theta = e_2^\theta + k_s e_1^\theta.\end{cases} \tag{9}$$

Then the final actuator controller is formulated as

$$u_\theta = [g_\theta]^{-1}\Big[-k_{\theta_1}|e_1^\theta|^{\frac{1}{3}}\mathcal{H}(e_1^\theta) - k_{\theta_2}|s_\theta|^{\frac{1}{2}}\mathcal{H}(s_\theta) + \vartheta_\theta - f_\theta\Big] \quad (10)$$

3.3.2 Stability Analysis

Theorem 1. Consider the nonlinear perturbated actuator system (4) and the designed control law u_θ given in (9). Then, the position tracking errors are globally finite-time stable at the origin.

Proof. we consider the stability proof of the position. The closed-loop dynamics for the position variable θ can be described as

$$\begin{cases} \dot{e}_1^\theta = e_2^\theta, \\ \dot{e}_2^\theta = -k_{\theta_1}|e_1^\theta|^{\frac{1}{3}}\mathcal{H}(e_1^\theta) - k_{\theta_2}|s_\theta|^{\frac{1}{2}}\mathcal{H}(s_\theta) + \varsigma_\theta, \\ \dot{\varsigma}_\theta = -k_{\theta_3}|e_1^\theta|^{0}\mathcal{H}(e_1^\theta) - k_{\theta_4}|s_\theta|^{0}\mathcal{H}(s_\theta) - \theta_d^{(3)}, \\ s_\theta = e_2^\theta + k_s e_1^\theta. \end{cases} \quad (11)$$

where $\varsigma_\theta = \vartheta_\theta - \ddot{\theta}_d$. The third expression in (10) can be associated with differential inclusion (DI) $\dot{\varsigma}_\theta \in -k_{\theta_3}|e_1^\theta|^{0}\mathcal{H}(e_1^\theta) - k_{\theta_4}|s_\theta|^{0}\mathcal{H}(s_\theta) + [-\lambda, \lambda]$. Therefore it is associated with DI $\dot{x} \in F(x)$ where the set valued map F is given by $F(x) = \left\{y \in \mathbb{R}^n | y = \left[e_2^\theta, \varsigma_\theta, \rho\right]^T\right\}$, for all $\rho \in -k_{\theta_3}|e_1^\theta|^{0}\mathcal{H}(e_1^\theta) - k_{\theta_4}|s_\theta|^{0}\mathcal{H}(s_\theta) + [-\lambda, \lambda] \subset \mathbb{R}$. This DI is homogeneous of degree $q_\theta = -1$ with weights $r_\theta = [3,2,1]^T$ [10].

Let the following candidate Lyapunov function be proposed for system (10)

$$V_\theta(e_1^\theta, e_2^\theta, \varsigma_\theta) = \alpha_1|e_1^\theta|^{\frac{5}{3}} + \alpha_2 e_1^\theta s_\theta + \alpha_3|s_\theta|^{\frac{5}{2}} + \alpha_4 e_1^\theta\left(|\varsigma_\theta|^2\mathcal{H}(\varsigma_\theta)\right) - \alpha_5 s_\theta \varsigma_\theta^3 + \alpha_6|\varsigma_\theta|^5, \quad (12)$$

where $\alpha_j = [\alpha_1, \dots, \alpha_6]^T \in \mathbb{R}^6, j = \overline{1,6}$ is a vector of coefficients. The time derivative of $V_\theta(e_1^\theta, e_2^\theta, \varsigma_\theta)$ is computed by

$$\begin{aligned} \dot{V}_\theta = \mathcal{M} &= \beta_1|e_1^\theta|^{\frac{4}{3}} + \beta_2 e_\theta \mathrm{sign}^{\frac{1}{2}}(s_\theta) \\ &- \beta_3 \mathrm{sign}^{\frac{2}{3}}(e_1^\theta)s_\theta \\ &+ \beta_4 \mathrm{sign}^{\frac{1}{3}}(e_1^\theta)\mathrm{sign}^{\frac{3}{2}}(s_\theta) + \beta_5|s_\theta|^2 \\ &- \beta_6 e_1^\theta \varsigma_\theta + \beta_7|e_1^\theta||\varsigma_\theta| \\ &- \beta_8 e_1^\theta \mathrm{sign}^0(s_\theta)|\varsigma_\theta| \\ &- \beta_9 \mathrm{sign}^{\frac{3}{2}}(s_\theta)\varsigma_\theta - \beta_{10} s_\theta \mathrm{sign}^2(\varsigma_\theta) \\ &+ \beta_{11}\mathrm{sign}^0(e_1^\theta)s_\theta|\varsigma_\theta|^2 \\ &- \beta_{12}|e_1^\theta||\varsigma_\theta|^2 - \beta_{13}\mathrm{sign}^{\frac{1}{3}}(e_1^\theta)\varsigma_\theta^3 \\ &- \beta_{14}\mathrm{sign}^{\frac{1}{2}}(s_\theta)\varsigma_\theta^3 + \beta_{15}|\varsigma_\theta|^4 \\ &+ \beta_{16}\mathrm{sign}^0(e_1^\theta)\mathrm{sign}^4(\varsigma_\theta) \\ &+ \beta_{17}\mathrm{sign}^0(e_2^\theta)\mathrm{sign}^4(\varsigma_\theta). \end{aligned} \quad (13)$$

where $\beta_1 = \alpha_2 k_{\theta_1}, \beta_2 = \alpha_2 k_{\theta_2}, \beta_3 = \frac{5}{3}\alpha_1, \beta_4 = \frac{5}{2}\alpha_3 k_{\theta_1}, \beta_5 = \frac{5}{2}\alpha_3 k_{\theta_2} - \alpha_2, \beta_6 = \alpha_2, \beta_7 = 2\alpha_4 k_{\theta_3}, \beta_8 = 2\alpha_4 k_{\theta_4}, \beta_9 = \frac{5}{2}\alpha_3, \beta_{10} = \alpha_4, \beta_{11} = 3\alpha_5 k_{\theta_3}, \beta_{12} = 3\alpha_5 k_{\theta_4}, \beta_{13} = \alpha_5 k_{\theta_1}, \beta_{14} = \alpha_5 k_{\theta_2}, \beta_{15} = \alpha_5, \beta_{16} = 5\alpha_6 k_{\theta_3}, \beta_{17} = 5\alpha_6 k_{\theta_4}$. The Lyapunov function V_θ given in (8) is homogeneous of degree $m = 5$. Thus, there exist a continuous homogeneous function $\mathcal{M}$ of degree $m + q_\theta = 4$ such that $\dot{V}_\theta \leq -\mathcal{M}$. Hence, there exist $\gamma_\theta > 0$ such that $\mathcal{M} \geq \gamma_\theta V_\theta^{\frac{4}{5}}$. Therefore $\dot{V}_\theta \leq -\gamma_\theta V_\theta^{\frac{4}{5}}$. This implies that the tracking error is finite-time stable at the origin. Furthermore, since the control system is homogeneous, the stability property is global. The expression of the settling-time can be obtained via solving the differential equation $\dot{V}_\theta \leq -\gamma_\theta V_\theta^{\frac{4}{5}}$. This can be achieved by utilizing the separation of variables method. Thus, by separating the variables and then integrating both sides of the equation we get $\int_0^t \frac{1}{V_\theta^{\frac{4}{5}}} dV_\theta \leq \int_0^t -\gamma_\theta dt$. Then, the following expression is obtained $5V_\theta^{\frac{1}{5}} \leq -\gamma_\theta t$. Finally, we can get $T_\theta \leq \frac{5}{\gamma_\theta} V_\theta^{\frac{1}{5}}$. It follows from Lemma 1 that the tracking error is finite-time stable. Thus, completing the proof.

4 SIMULATION RESULTS AND DISCUSSIONS

4.1 Control Gain Tuning

The gains of the controller are tuned by using the *"Optimization Toolbox"*. Two blocks are used to optimize the parameters: *(i)* Check Step Response Characteristics (CSRC) block; *(ii)* Check Against Reference (CAR) block. In the general case, these

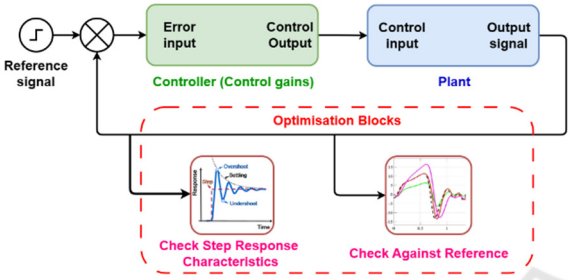

Figure 1: Optimization blocks integration.

two optimization blocks are inserted in the output of the control loop (Fig.4). The CSRC block checks that a signal satisfies the step response bounds during simulation (Settling-time, Rise-time, % Overshoot, and % Undershoot). CAR block checks that a signal remains within the tolerance bounds, at steady-state, of a reference signal during the simulation.

CSRC, CAR blocks ensure that a signal remains within specified time-domain characteristic bounds. In our case, these bounds are chosen for a unit step response, as shown in Table 1.

4.2 Controller Performances

In this section, to visualize and extract the performance of the proposed controller, we will test its step response by using a step of 30-degree amplitude as the desired signal at the input of the system. Fig.5 shows the response of our system when using the proposed controller and two other controllers.

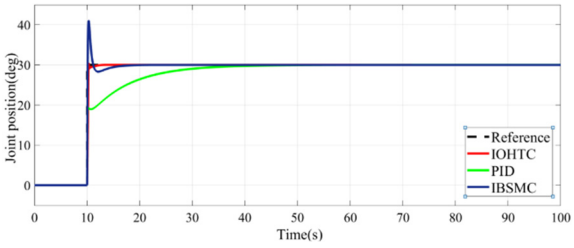

Figure 2: Step response.

Fig.5 clearly shows the advantages of the proposed controller compared to the two other implemented controllers (PID and IBSSMC). IOHTC showed better performance with a response time t_{IOHTC}=0.22s without overshoot, while PID has a response time t_{PID}>25s, and IBSSMC has a considerable overshoot D_{IBSSMC}>33% which can imply risks on the user (the non-respect of the limits of articular movements).

4.3 Ankle Angular Position Tracking During Gait

This section will test the proposed controller using real walking data. These data have been derived from a publicly available dataset (Embry, 2018); from this dataset, we have recovered the evolution of the angular position of the ankle during a real walk on flat ground with a speed of 1m/s. This test allows us to visualize the proposed controller's performance and the two other implemented controllers in real ankle joint movement tracking problem.

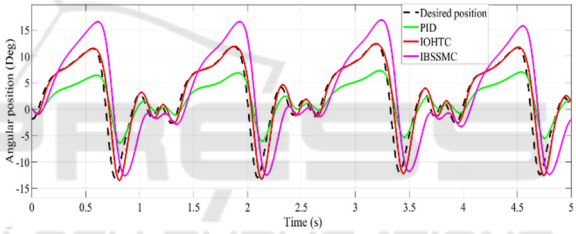

Figure 3: Ankle movement tracking during real gait.

In order to clearly show the difference between the system responses using each controller, we took a portion of data equivalent to four gait cycles and used it as a reference signal. Figures 6 and 7 show the desired angular position tracking and the evolution of the error over time. Finally, we use RMSE as a metric to compare the three controllers. The proposed controller showed better performance with RMSE=0.2509 deg, the PID controller has RMSE=0.8492 deg, and the IBSSMC has RMSE=0.5613 deg.

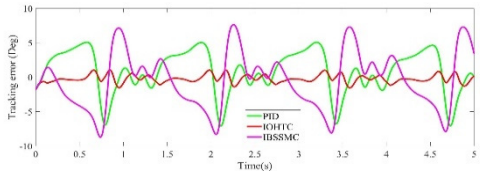

Figure 4: Tracking error evolution over the time.

Table 1: Specified time-domain characteristic bounds for position states.

State	Optimization Block	Characteristics	Value
θ	CSRC	Settling-time (s)	≤ 2 s
		Rise-time (s)	≤ 4 s
		Overshoot (%)	≤ 30 %
		Undershoot (%)	≤ 5 %
	CAR	Amplitudes	$1 - \exp(-\text{linspace}(0,20)/2)$
		Absolute tolerance	$\text{eps}^{(1/3)}$
		Relative tolerance	0.01

Several simulations using the previously implemented controllers were performed on the ankle exoskeleton robot SOLIDWORKS model using simscape multibody link. The tests performed allowed us to validate the model designed model, and the simulations show that the ankle of the model performs movements similar to a human ankle during walking.

5 CONCLUSION

This work aims to achieve two main tasks for implementing a robot exoskeleton: design and control. Regarding the design part, an ankle exoskeleton robot was designed using SOLIDWORKS, considering all the essential points for the robot to be comfortable, lightweight and secure. Concerning the designed exoskeleton control, we proposed an IOHTC approach to design a robust exoskeleton angular position control. The stability of the control system has been rigorously discussed based on a homogeneous-Lyapunov function. Results based on the real-data gait ankle angular position tracking simulation are found to be consistent with the theoretical foundations. A comparative analysis based on various performance indices was performed to thoroughly examine the synthesised controller's capabilities. Results witness the effectiveness and superiority of the proposed control law. Further studies will address realizing the proposed exoskeleton robot and real-world experiment and the exploration of the development of EMG-based model for intelligent control of this exoskeleton robot.

REFERENCES

Alvarez-Perez, M. G.-M.-S. (2020). Robot-assisted ankle rehabilitation: A review. *Disability and Rehabilitation: Assistive Technology,*, 15(4), 394-408.

Bortole, M. V.-V. (2015). The H2 robotic exoskeleton for gait rehabilitation after stroke: early findings from a clinical study. *Journal of neuroengineering and rehabilitation*, 12, 1-14.

De Looze, M. P. (2016). Exoskeletons for industrial application and their potential effects on physical work load. *Ergonomics*, 671-681.

Embry, K. V. (2018). The effect of walking incline and speed on human leg kinematics, kinetics, and EMG. . *IEEE DataPort*, 10.

Falcón, R. R. (2019). Comparative analysis of continuous sliding-modes control strategies for quad-rotor robust tracking. . *Control Engineering Practice*, 90, 241-256.

Falcón, R., Ríos, H., & Dzul, A. (2019). Comparative analysis of continuous sliding-modes control strategies for quad-rotor robust tracking. *Control Engineering Practice, 90*, 241-256.

Farris, D. J. (2023). A systematic literature review of evidence for the use of assistive exoskeletons in defence and security use cases. *Ergonomics*, 61-87.

Jimenez-Fabian, R. &. (2012). Review of control algorithms for robotic ankle systems in lower-limb orthoses, prostheses, and exoskeletons. *Medical engineering & physics*, 34(4), 397-408.

Lee, T. K. (2021). Design of a 2dof ankle exoskeleton with a polycentric structure and a bi-directional tendon-driven actuator controlled using a pid neural network. In Actuators . *MDPI*, (Vol. 10, No. 1, p. 9).

Mechali, O. X. (2022). Fixed-time nonlinear homogeneous sliding mode approach for robust tracking control of multirotor aircraft: Experimental validation. , . *Journal of the Franklin Institute*, 359(5), 1971-2029.

Messaoui, A. M. (2023). Robust Finite-Time Control of a Multirotor System via an Improved Optimized Homogeneous Twisting Control: Design and Validation. *International Conference on Simulation and Modeling Methodologies, Technologies and Applications.*, (pp. 326-331). Rome, Italy.

Mubin, O. A. (2019). Exoskeletons with virtual reality, augmented reality, and gamification for stroke patients' rehabilitation: systematic review. *JMIR rehabilitation and assistive technologies*, e12010.

Plaza, A. H. (2021). Lower-limb medical and rehabilitation exoskeletons: A review of the current designs. *IEEE Reviews in Biomedical Engineering*, 102554.

Pont-Esteban, D. S.-U. (2022). Robust Motion Control Architecture for an Upper-Limb Rehabilitation Exosuit. *IEEE Access*, 10, 113631-113648.

Xu, Q. (2017). Continuous integral terminal third-order sliding mode motion control for piezoelectric

nanopositioning system. *IEEE/ASME Transactions on Mechatronics*, 22(4), 1828-1838.

Zhao, J. Y. (2021). Sliding mode control combined with extended state observer for an ankle exoskeleton driven by electrical motor. *Mechatronics*, 76, 102554.

Zhou, J. Y. (2021). Lower limb rehabilitation exoskeleton robot: A review. *Advances in Mechanical Engineering*, 13(4), 16878140211011862.